Volume 24, No 2 | International Journal of Radiation Research, April 2026

Evaluation of ^{68}Ga-PSMA PET/CT in the staging of patients with prostate cancer

M.M.M. Shehata*, H.A. Kader Morsy, R.S.E. Hussein, A.A.M. Okba

Department of Diagnostic Radiology, Faculty of Medicine, Ain Shams University, Cairo, Egypt

► ***Original article***

Corresponding author:
Mahmoud M.M. Shehat, M.Sc.,
E-mail:
mahmoud.shehata007@gmail.com

Received: January 2025
Final revised: October 2025
Accepted: November 2025

Int. J. Radiat. Res., April 2026; 24(2): 397-403

DOI: 10.61186/ijrr.24.2.14

Keywords: *Prostate cancer, prostate-specific membrane antigen, prostate-specific antigen density, 68Ga-PSMA PET/CT.*

ABSTRACT

Background: Targeting prostate-specific membrane antigen (PSMA), with Gallium-68 PSMA-directed Positron Emission Tomography/Computed Tomography (^{68}Ga-PSMA PET/CT) is advanced imaging technique for prostate cancer (PCa) diagnosis. The current study evaluated the performance of ^{68}Ga-PSMA PET/CT for staging and follow-up of PCa patients. ***Material and Methods:*** 54 newly diagnosed (Group I) and 66 recurrent PCa patients (Group II) underwent estimation of serum total prostate-specific antigen (PSAT), calculation of PSA density (PSAD), and grading by the Gleason grading system. After obtaining the whole-body images using the integrated PET/CT scanner, Discovery IQ five-ring machine, and PET scanning, the maximum standardized uptake (SUV-max) values were calculated. Histopathology is the gold standard for assessment of the diagnostic performance of ^{68}Ga-PSMA PET/CT for Group II. ***Results:*** The PSAT levels and density for Group I increased progressively with Gleason grade, with significant (P=0.021 and P=0.005, respectively) differences among grades. The lymph nodes and local tumor SUV-max were remarkably higher (P<0.001 & 0.01) in Group I. The SUV-max according to PSAT grades of Group I patients showed a significant (P<0.001) difference. There was positive, significant (P<0.001) relation between PSAD and SUV-max. The regression model for PSAD versus SUV-max was significant. The natural log of SUV-max increased by 2.03-fold with each fold increase in the natural log of PSAD. ***Conclusion:*** Integrating ^{68}Ga-PSMA PET/CT in the diagnostic workup for PCa patients helps the management decision-making and is particularly valuable for lesions in areas inaccessible for biopsy, or if PSA levels are in the diagnostic gray-zone.

INTRODUCTION

Prostate cancer (PCa) is one of the common malignant diseases affecting males and most commonly leads to an elevated frequency of other morbidities, and deleteriously affects men's health [1]. Prostate-specific antigen (PSA) is a minimally invasive serum test for diagnosing and monitoring PCa. However, PSA showed limited diagnostic performance, with subsequently increased frequency of invasive biopsies, overtreatment of indolent disease, and the need for more accurate diagnostic and prognostic methods [2]. The PSA density (PSAD) which relates the estimated level of serum PSA to the prostatic volume as judged by transrectal ultrasound (TRUS). PSAD (ng/mL^2) informs biopsy decisions better than PSA alone [3]. The decisions for biopsy-taking align with the value of PSAD calculated using combined trans-perineal and transabdominal US versus the triplane MRI-calculated PSAD. Therefore, US-PSAD may be applied to obtain an accurate PSAD and for planning other investigations [4].

However, prostate biopsy should not be avoided if the PSAD value exceeded 0.15 ng/mL^2 and the calculated ratio between the free and total PSA levels was less than 0.15 [5]. In cases with a grey-zone level of PSA, the application of PSAD and the PI-RADS improved the diagnostic yield [6]. The prostate-specific membrane antigen (PSMA) is one of the transmembrane proteins that characterize the prostatic tissue and is overexpressed on the surface of most of its tumor cells [7]. The increased expression levels of PSMA in malignant cells enable its targeting for both diagnostic imaging and therapeutic intervention. PSMA opened the scale for therapies that can mitigate the levels of PSA, improve the disease-free survival time, and patients' quality of life [8]. Gallium-68(^{68}Ga)-PSMA-11 directed Positron Emission Tomography/Computed Tomography [^{68}Ga]Ga-PSMA-11 PET/CT is an emerging diagnostic modality that reflects PSMA expression at metastatic sites [9]. The current study, through the comparison of findings of patients with de novo or recurrent PCa, establishes the utility of ^{68}Ga-PSMA PET/CT for the diagnosis and follow-up of PCa.

This work tried to evaluate the performance of the ^{68}Ga-PSMA PET/CT for the staging and as a modality for follow-up of PCa patients.

[DOI: 10.61186/ijrr.24.2.14]

MATERIALS AND METHODS

Study population

Males older than 50 years, suspicious of having PCa on digital rectal examination, and who had a total PSA serum level higher than 4 ng/ml were eligible for evaluation. The collected data included demographic, clinical, and lab data. The findings of the US-guided prostatic biopsy and the histopathological diagnosis were included. The detected lesions were graded according to the Gleason grading of PCa [10]. Based on the results obtained by Berger *et al.* [11], the number of enrolled patients was 30 (NCSS PASS 11.0).

Inclusion and Exclusion criteria

Patients with a prostatic mass found during routine ultrasound, confirmed by CT/MRI and diagnosed as intermediate or high-risk PCa based on transrectal US-guided biopsy were enrolled. Additionally, patients who previously received treatment for PCa and developed newly suspicious clinical or radiological findings during regular follow-up were also included.

Patients who underwent prostate surgery or received radiotherapy or androgen deprivation therapy within 4 weeks, or who received chemotherapy within two weeks, or whose histopathological diagnosis was missed were excluded from the study.

Ethical approval

The Ethics Committee at Ain Shams University approved the study protocol (registered number M D182/2021, on 17/09/2021). Patients accepted to participate signed an informed written consent after being informed of the procedure details before inclusion in this study.

Preprocedural requirements

Serum PSA level and GFR measurement must be assessed within two weeks before the scanning procedure. The procedure had to be postponed for two and four weeks after the last dose of chemotherapy and radiotherapy, respectively.

Preprocedural preparation

Oral hydration and an open venous access were mandatory before the 68 Ga PSMA injection. An intravenous bolus dose injection of 1.8-2.2 MBq/kg was followed by a post-injection flush with 10 ml of 0.9% saline. Patients must void immediately before scanning to reduce pitfalls of radiotracer concentration in the urinary bladder.

Image acquisition

Sixty minutes after the radiotracer injection, whole-body images were obtained using the integrated PET/CT scanner Discovery IQ five-ring machine, a class I IPX0 device with 16 slices of CT (General Electric Company, Milwaukee, Wisconsin, USA). Patients were supine positioned on the scanner table, and a CT scan with/without intravenous contrast enhancement was acquired with a tube current (130 kVp, 48–76 mAs), a slice thickness of 4.0 mm, 0.6 s gantry rotation, and a collimator width of 6×3 mm. For contrast-enhanced studies, iodinated non-ionized contrast material as Omnipaque was administered using an automated injector, in a dose of 1.5 ml/kg, at a rate of 3-4 ml/sec. Then, PET scanning with a duration of 3 minutes per bed position was performed with the identical transverse field of view in the caudocranial direction. The duration of the full procedure was about 20-30 minutes.

Image interpretation

The regions of interest were marked, with avoidance of the bladder and metastatic lesions, to calculate the maximum standardized uptake value (SUV-max). The highest SUV-max values from the whole prostate gland and distant lesions were considered to be the most expressing PSMA sites. Primary and metastatic lesions were suspected when these sites took up more tracer than the adjacent tissue. Images were analyzed both visually and semi-quantitatively by measuring the SUV-max of the primary prostatic tumor and metastatic lesions.

Validation and reference standard

The diagnostic accuracy of 68Ga-PSMA PET/CT for disease staging and follow-up was validated against histopathological findings, which were considered the gold standard. Histopathological confirmation was obtained from prostate biopsy or radical prostatectomy specimens whenever available. In patients who did not undergo surgical resection, the reference standard included a combination of clinical, biochemical, and radiological follow-up data, such as serial PSA levels, multiparametric MRI findings, and treatment response assessment.

This approach is consistent with previously published studies validating the performance of PSMA PET/CT using histopathology as the reference standard by Berger *et al.* [11] and Li *et al.* [21].

Statistical analysis

Data were described as percentages and mean (±SD). The categorical variables were assessed by the Chi-square test and Fisher's exact test. The comparisons for the numerical variables and defining the significance of the differences among the studied groups were done by the Mann-Whitney test in case of violation of parametric assumptions, whereas comparing numerical variables among more than three groups was done by the Kruskal-Walli's test. Kendal Tau test of correlation was applied to find the correlation between two numerical variables, then simple linear regression was used to find the mathematical relation between these variables, which was transformed logarithmically to achieve the

[DOI: 10.61186/ijrr.24.2.14]

linear relation between variables and to be suitable for the calculations of the linear regression. Then, pseudo-R-squared is used to show the percentage of variation. Statistical analysis was done using R-version-4.3.1. P<0.05 indicated significance.

RESULTS

This study entailed a preliminary evaluation of 133 patients; 13 patients were excluded for either low GFR (n=8) or missed results of histopathological diagnosis of the obtained biopsies (n=5). The study included 54 patients aged 67.3 (±9.5) years with newly diagnosed PCa (Group I) and 66 patients aged 70 (±8.1) years with recurrent lesions detected during follow-up (figure 1).

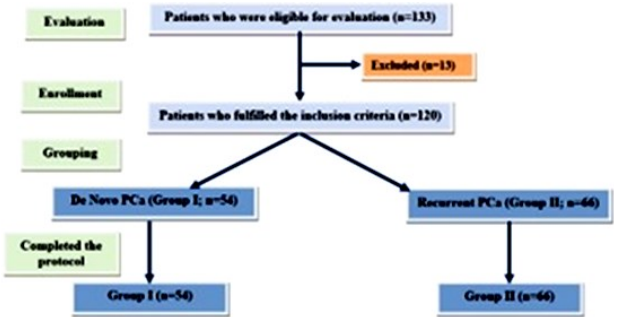

Figure 1. study flow chart.

Among cases in both study groups, thirty-five patients (29.2%) were graded as 4 on the Gleason grading system, and 28 patients (23.3%) were scored as 3, while another twenty-eight patients (23.3%) were scored as 2. Twenty-one patients (17.5%) were scored 1, and eight patients (6.7%) were scored as 5. The frequency of the studied patients among the scores of the Gleason grading system showed an insignificant difference between the study groups (P=0.256). Seventy-seven patients (64.2%) were free of lymph node metastasis, twenty-two patients (18.3%) had local nodal metastasis, and twenty-one patients (17.5%) had metastasis in local and distant nodal metastasis. Patients' grouping according to LN status showed a significant (P=0.014) intergroup difference.

The estimated levels of total PSA (PSAT) were markedly elevated in samples from patients in group 1 (P=0.001). However, the density of PSAT was insignificantly (P=0.058) higher in patients of Group II.

Patients' grouping according to PSAT defined seventy-two patients (60%) who were grouped as PAST4 with a mean PSAT of <0.5 ng/ml, nineteen patients (15.8%) who were grouped as PAST1, and twenty-five patients (20.8%) were grouped as PSAT3, while only four patients (3.4%) were of PAST2. Patients' grouping according to PAST showed a significant (P=0.0001) intergroup difference.

PET/CT defined thirty patients (25%) who had multiple bone metastases, ten patients (8.3%) had solitary bone metastasis, and six patients (5%) had oligo bone metastasis, while the imaging of the remaining seventy-four patients (61.7%) was negative. Patients' distribution according to bone metastasis identification showed a non-significant (P=0.062) difference between groups. The values of the SUV-max were considerably higher in group 1 cases (P=0.002, 0.017 and <0.001) for the nodal and bony metastatic lesions and for the local prostatic lesion (table 1).

Table 1. The findings of investigations performed for the enrolled patients.

Findings		Group	I (n=54)	II (n=66)	P-value	significance
Gleason grading system score		1	12 (22.2%)	9 (13.6%)	0.256*	NS
		2	13 (24.1%)	15 (22.7%)		
		3	8 (14.8%)	20 (30.3%)		
		4	16 (29.6%)	19 (28.8%)		
		5	5 (9.3%)	3 (4.6%)		
Frequency according to LN status		Negative	29 (53.7%)	48 (72.7%)	0.014*	S
		Local	16 (29.6%)	6 (9.1%)		
		Local and distant	9 (16.7%)	12 (18.2%)		
PSA data	Total level		69.5±151.1	33.6±87.22	0.001‡	HS
	Patients' frequencies according to the estimated levels of total PSA (ng/ml)	PSAT4 [<0.5]	30 (55.6%)	42 (63.64%)	0.0001**	HS
		PSAT1 [0.5-1]	3 (5.6%)	16 (24.24%)		
		PSAT3 [1-2]	20 (37%)	5 (7.58%)		
		PSAT2 [>2]	1 (1.8%)	3 (4.55%)		
	PSAD		0.72±1.26	0.87±1.88	0.058‡	NS
Bone Mets (PET/CT)		Negative	40 (74.07%)	34 (51.5%)	0.062**	NS
		Multiple	9 (16.67%)	21 (31.8%)		
		Solitary	4 (7.41%)	6 (9.1%)		
		Oligo	1 (1.85%)	5 (7.6%)		
SUV Max	Lymph nodes		15.88±5.9	9.82±7.92	0.002‡	HS
	Bone metastasis		10.69±5.95	9.1±11.27	0.017‡	S
	Local tumor		14.88±11.09	8.3±15.38	0.0001‡	HS

LN: Lymph node; PSA: Prostate-specific antigen; PSAD: PSA density; SUV-max: maximum standardized uptake value; NS: non-significant; S: Significant; HS: Highly significant *Chi square test, **Fisher exact test, ‡Mann Whitney test.

[DOI: 10.61186/ijrr.24.2.14]

The PSAT levels and density in patients of Group I increased progressively with Gleason grade, with remarkable (P=0.021 and P=0.005) differences between both variables according to the Gleason grade. The frequency of lymph nodal and bone metastasis varied with Gleason grade, showing significant differences for both lymph nodal (P=0.044) and bony (P=0.025) metastasis. The variation in PSAT density and lymph nodal metastasis according to Gleason grade was not significant (P=0.396 and P=0.394, respectively) in Group II, but the frequency of bone metastasis by Gleason grade in Group II was significant (P=0.018) (table 2).

Table 2. Distribution of PSAT, lymph nodal, and bone metastasis according to the Gleason grade of patients of both groups.

Group	Gleason grade Items		1	2	3	4	5	P value	significance
I	PSAT (ng/ml)	Level	17.2±9.5	27.9±26	32.1±32.2	147.7±251.4	146.3±170	0.021*	S
		density	0.2±0.13	0.39±0.28	0.35±0.19	1.4±1.91	1.42±1.94	0.005*	HS
	Lymph node metastasis	Negative	10 (90.9%)	7 (58.3%)	2 (28.6%)	5 (33.3%)	1 (20%)	0.044**	S
		Local	0 (0%)	4 (33.3%)	3 (42.9%)	6 (40%)	3 (60%)		
		Local and Distant	1 (9.1%)	1 (8.3%)	2 (28.6%)	4 (26.7%)	1 (20%)		
	Bone metastasis	Negative	10 (90.9%)	9 (75%)	5 (71.4%)	10 (66.7%)	2 (40%)	0.025**	S
		Solitary	1 (9.1%)	2 (16.7%)	1 (14.3%)	0 (0%)	0 (0%)		
		Oligo	0 (0%)	1 (8.3%)	0 (0%)	0 (0%)	0 (0%)		
		Multiple	0 (0%)	0 (0%)	1 (14.3%)	5 (33.3%)	3 (60%)		
II	PSAT (ng/ml)	density	0.21±0.3	0.6±1.36	0.39±0.32	1.42±2.77	2.38±3.16	0.396*	NS
	Lymph node metastasis	Negative	8 (88.9%)	14 (70%)	13 (86.7%)	11 (57.9%)	1 (50%)	0.394**	NS
		Local	0 (0%)	1 (5%)	1 (6.7%)	4 (21.1%)	0 (0%)		
		Local and Distant	1 (11.1%)	5 (25%)	1 (6.7%)	4 (21.1%)	1 (50%)		
	Bone metastasis	Negative	6 (66.7%)	11 (55%)	11 (73.3%)	6 (31.6%)	0 (0%)	0.018**	S
		Solitary	1 (11.1%)	3 (15%)	1 (6.7%)	1 (5.3%)	0 (0%)		
		Oligo	1 (11.1%)	2 (10%)	0 (0%)	0 (0%)	1 (50%)		
		Multiple	1 (11.1%)	4 (20%)	3 (20%)	12 (63.2%)	1 (50%)		

PSAT: Total prostatic-specific antigen; NS: non-significant; S: Significant; HS: Highly significant; *Kruskal Wallis test; **Fisher exact test.

The SUV-max according to PSAT grades of Group I patients was significantly (P<0.001) different. However, LN SUV-max according to the location of LN metastasis, either local lymph nodes or both local and distant lymph nodal metastasis, showed an insignificant (P=0.507) difference. Also, bone metastasis SUV max showed an insignificant (P=0.651) difference between SUV max for patients who had local bone metastasis and those who had both local and distant bone metastasis (table 3).

Table 3. The SUV-max levels among PSAT grades, and the site of lymph nodal, and bone metastasis.

Variables		SUV max	P value	Significance
PSA total	PSAT1	1.44±1.41	<0.001*	HS
	PSAT2	3.2±3.3		
	PSAT3	3.98±2.98		
	PSAT4	11.79±18.38		
Lymph node metastasis	Local	10±7.54	0.507**	NS
	Local and Distant	9.73±8.47		
Bone metastasis PET/CT	Local	21.78±29.37	0.651**	NS
	Local and Distant	15.85±25.76		

The relation between PSA density and SUV max showed a positive, significant (P<0.001) correlation with a coefficient equal to 0.38 (table 4, figure 2).

The natural log of the PSAD and SUV max was calculated, and then a regression model for PSAD versus SUV max was used to quantify the effect of PSA density on SUV max. This analysis model was significant and indicated an increase in the natural log of SUV max by 2.03-fold with each fold increase in the natural log of PSAD, and this indicates a significant impact of PSAD on the SUV max. The Pseudo R-Square is 0.25%, and the variation in the SUV max by 25% can be attributed to variation in PSAD.

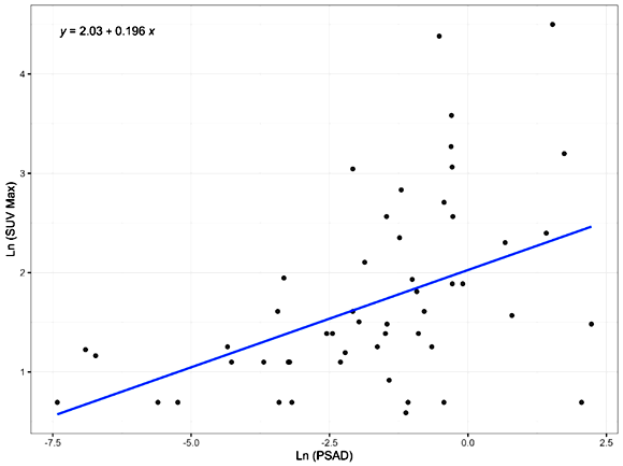

Figure 2. Scatter diagram showing the relation between SUV Max (maximum standardized uptake value) and PSDA (prostate specific antigen density).

Table 4. Regression and Correlation of PSAD and SUV max in Group I.

Log (SUV max)	Regression*			Correlation**	
	Estimate	P value	PseudoR2	Correlation	P value
Intercept	2.03	<0.001 (HS)	0.25	0.38	<0.001 (HS)
Log (PSAD)	0.20	<0.001 (HS)			

Case presentation

Representative clinical cases are presented to illustrate the diagnostic role of 68Ga-PSMA PET/CT in the staging and follow-up of prostate cancer patients. Each case highlights the metabolic and anatomic imaging findings, with corresponding numbered figures and detailed, self-explanatory captions.

[DOI: 10.61186/ijrr.24.2.14]

Case I

A 74-year-old male patient with a history of prostate cancer (Gleason score 8 [4+4], grade group 4) and PSA level of 234 ng/mL. Pathological examination of the harvested biopsy confirmed the diagnosis. Following chemotherapy and hormonal treatment, a 68Ga-PSMA PET/CT scan was performed with an administered activity of 275.2 MBq.

Findings

No PSMA-avid lesions were detected in the prostate or regional lymph nodes. Multiple PSMA-avid osseous metastases were observed involving the axial and appendicular skeleton, with a maximum standardized uptake value (SUVmax) reaching 33 at the lumbar vertebrae.

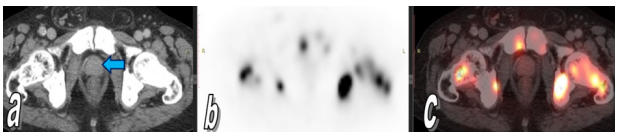

Figure 3. Axial PSMA PET/CT images [**(a)** CT, **(b)** PET and **(c)** fused PET/CT] of the pelvis showing an average-sized prostate gland (arrow) without significant PSMA uptake, indicating no local recurrence.

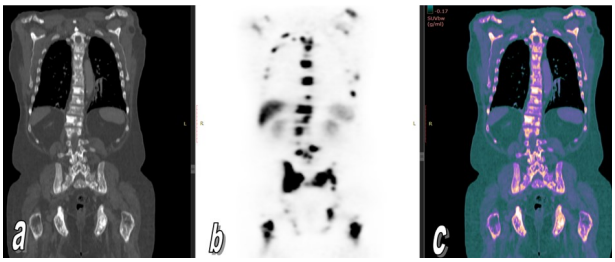

Figure 4. Reformatted coronal PET/CT images [**(a)** CT, **(b)** PET and **(c)** fused PET/CT] through the spine demonstrating multiple intensely PSMA-avid osseous lesions consistent with widespread skeletal metastases.

Figure 5. Maximum Intensity Projection (MIP) image revealing disseminated PSMA-avid osseous metastases throughout the skeleton, confirming diffuse metastatic disease.

Case II

A 60-year-old male presented with lower urinary tract symptoms and hepatic focal lesions suggestive of metastases on conventional CT. Initial prostate biopsy confirmed prostate cancer, though the PSA level was low (1.2 ng/mL). A 68Ga-PSMA PET/CT scan was performed with an administered activity of 315.2 MBq.

Findings

Axial PET/CT images demonstrated a markedly enlarged prostate gland with irregular outlines, indentation of the bladder base, and suspected invasion of the right vesicoureteric junction and anterior rectal wall. The lesion showed only faint PSMA uptake (SUVmax = 2.4), inconclusive for malignancy.

Multiple enlarged iliac lymph nodes showed no significant PSMA avidity. The liver demonstrated multiple confluents, variably sized, heterogeneously enhancing focal lesions that were cold (non–PSMA-avid) on PET imaging. Re-evaluation of the biopsy confirmed the diagnosis of transitional cell carcinoma (TCC) rather than prostate adenocarcinoma.

Figure 6. Axial PET/CT images [**(a)** CT, **(b)** PET and **(c)** fused PET/CT] of the pelvis showing an enlarged prostate with irregular margins (red arrow) and low-grade PSMA uptake (SUVmax = 2.4).

Figure 7. Axial PET/CT images [**(a)** CT, **(b)** PET and **(c)** fused PET/CT] of the pelvis revealing multiple enlarged iliac lymph nodes (arrows) without significant PSMA uptake.

Figure 8. Axial PET/CT images [**(a)** CT, **(b)** PET and **(c)** fused PET/CT] of the liver demonstrating multiple large hypodense focal lesions (arrows) with no PSMA avidity (“cold lesions”), indicating non-prostatic metastases.

Figure 9. MIP image of the whole body showing no PSMA-avid lesions, only multiple cold hepatic focal lesions corresponding to TCC metastases.

DISCUSSION

The disease was more aggressive in de novo cases (Group I) than in recurrent cases (Group II), as indicated by a significantly higher frequency of local and distant nodal metastasis, and a non-significantly higher frequency of detected bony metastases. However, patients’ distribution based on the Gleason grading system, estimated levels of total PSA (PSA), and the calculated PSA density (PSAD) showed

[DOI: 10.61186/ijrr.24.2.14]

negligible differences between the groups. These findings highlight the need for further diagnostic and differentiating studies, and support the value of the combined application of other diagnostic approaches with PSA metrics.

These findings align with Gurbuz *et al.* [12], who found that preoperative and pathological Gleason scale discordantly graded about 50% of PCa patients undergoing radical prostatectomy, relative to pathological examinations of the excised specimens. Jin *et al.* [13] documented that the use of MRI in conjunction with serum PSA levels allowed proper stratification of PCa patients, supported valuable decision-making pathways for the management of clinically significant prostate cancer (csPCa), and helped biopsy sparing. Quarta *et al.* [14] reported that the detection of csPCa in cases with tumors graded as PI-RADS 3 might be improved by the use of combined determination of PSAD and index lesion location on the multiparametric magnetic resonance imaging, particularly in the peripheral and the transitional zones.

Fortunately, the calculated SUV-max for the lymph nodes and local tumor was remarkably elevated in Group I patients, thereby differentiating these patients' categories and identifying the patients with higher risk. Moreover, for patients with de Novo PCa, the SUV max showed a significant difference among PSAT grades, with a significant positive correlation with PSAD. Regression analysis showed an increase in the natural log of SUV max by 2.03-fold with each increase in the natural log of PSAD by one-fold, indicating a significant impact of PSAD on the SUV max.

In line with the current data, Heetman *et al.* [15] documented the inclusion of SUV max to improve the goodness of diagnosis of patients with ISUP-Grade Group ≥2 and ≥3 for its significantly high statistical performance. Also, Pepe *et al.* [16] documented strict follow-up using SUV max for patients with PI-RADS score-5, and negative pathological examination to allow diagnosis of csPCa, especially with downgrading PI-RADS score on multiparametric MRI (mpMRI) of the prostate.

Moreover, Chen *et al.* [17] found that integrating [^{68}Ga] Ga-PSMA PET/CT SUV-max with prostate health index increased the accuracy of diagnosing csPCa in patients who had PSA levels ≥20 ng/mL and biopsy-free, with an AUC of 0.951, and provides a valuable noninvasive diagnostic modality that can spare biopsies and improve patient care. Li *et al.* [18] reported improved clinical decision-making with enhanced diagnostic accuracy by incorporating SUV-max with the ratio of serum PSA over other individual conventional metrics, and mitigating the frequency of unnecessary biopsies, especially for men with PI-RADS ≤ 3 MRI results. Wang *et al.* [19] documented that coupling SUV-max with prostate health index achieved AUCs of 0.955 to diagnose cases of PI-RADS ≥ 4, with a reduction of biopsy rate by 92.41%, while missing only 1.53% of csPCa cases in this high-risk population.

Furthermore, Falkenbach *et al.* [20] documented that the implementation of [^{68}Ga]Ga-PSMA PET/CT SUV max of metastatic tissue with the ratio of diameter to volume was related to the higher contributory role for PSA for metastatic spread of PCa in patients reported to have minute metastatic lesion that might secrete indetectable amounts of PSA to indicate biochemical recurrence. Li *et al.* [21] found that false negatives occur in cases having simple atrophy with cyst formation due to the overexpression of PSMA in these lesions as documented histologically. They also reported that false positives can be differentiated from true ones by having significantly lower SUV values.

***Limitations*:** This is a single-center study, and the sample size is relatively small limiting the generalizability of the outcomes. Larger multicenter comparative studies involving a broader patient population are mandatory to establish the implementation of ^{68}Ga-PSMA PET/CT in the diagnostic armamentarium for PCa cases.

CONCLUSION

The obtained data highlight the importance of integrating ^{68}Ga-PSMA PET/CT for the diagnosis of PCa patients. The importance of ^{68}Ga-PSMA PET/CT is particularly evident in cases of suspected lesions located in areas inaccessible for biopsy, in patients showed gray-zone PSA levels, and those at high anesthetic risk.

***Acknowledgment*:** The authors thank the staff of the Department of Radiology and Nuclear Medicine, [Ain Shams University], for their valuable support in data collection and image acquisition.

***Funding*:** This research did not receive any specific grant from funding agencies in the public, commercial, or not-for-profit sectors.

***Conflict of interest*:** The authors declare no conflict of interest.

***Ethical consideration*:** Approved by the Ethics Committee at Ain Shams University approved the study protocol. (Approval No. [M D182/2021], Date: [17/09/2021]). Written informed consent was obtained from all participants.

***Author contributions*:** M.M.M.S., was responsible for conceptualization, methodology, investigation, data curation, original draft writing, and visualization. H.A.K.M., contributed to formal analysis, validation, supervision, and the review and editing of the manuscript. R.S.E.H., participated in resource provision, data acquisition, literature review, and manuscript review and editing. A.A.M.O., performed the statistical analysis, project administration,

[DOI: 10.61186/ijrr.24.2.14]

manuscript review and editing, and provided final approval of the manuscript. All authors have read and approved the final version of the manuscript and agree to be accountable for all aspects of the work.

***AI assistance*:** No AI tools were involved in data analysis, image interpretation, or result generation.

REFERENCES

1. Xu Z, Chen X, He Y, Tong J, Chen C, Ding M, *et al.* (2025) The potential biological function of STARD8 in prostate cancer: A bioinformatic and experimental validation study. *Biochim Biophys Acta Mol Basis Dis,* ***1871****(6): 167897*.
2. Crocetto F, Musone M, Chianese S, Conforti P, Selvaggio G, Caputo V, *et al.* (2025) Blood and urine-based biomarkers in prostate cancer: current advances, clinical applications, and future directions. *J Liq Biopsy,* ***9****: 100305*.
3. Nordström T, Akre O, Aly M, Grönberg H, Eklund M (2018) Prostate -specific antigen (PSA) density in the diagnostic algorithm of prostate cancer. *Prostate Cancer Prostatic Dis,* ***21****(1): 57-63*.
4. Pantelidou M, Caglic I, George A, Blyuss O, Gnanapragasam V, Barrett T (2022) Evaluation of transabdominal and transperineal ultrasound-derived prostate specific antigen (PSA) density and clinical utility compared to MRI prostate volumes: a feasibility study. *PLoS One,* ***17****(9): e0274014*.
5. Bostancı C and Demir DÖ (2024) The effect of the combination of prostate-specific antigen derivatives with multiparametric prostate magnetic resonance imaging scores on the negative predictive value of it in grey zone patients. *Actas Urol Esp (Engl Ed),* ***48****(3): 238-245*.
6. Wen J, Liu W, Shen X, Hu W (2024) PI-RADS v2.1 and PSAD for the prediction of clinically significant prostate cancer among patients with PSA levels of 4–10 ng/ml. *Sci Rep,* ***14****(1): 6570*.
7. Diao W, Cai H, Chen L, Jin X, Liao X, Jia Z (2019) Recent advances in prostate-specific membrane antigen-based radiopharmaceuticals. *Curr Top Med Chem,* ***19****(1): 33-56*.
8. Wang L, Lu C, Wang X, Wu D (2025) PSMA-targeted therapy: from molecular mechanisms to clinical breakthroughs in castration-resistant prostate cancer. *Eur J Med Chem,* ***296****: 117829*.
9. Pepe P, Pepe L, Cignoli D, Roscigno M (2025) PSMA PET/CT in the diagnosis of prostate cancer: why and when? *Arch Ital Urol Androl,* ***97****(2): 13746*.
10. Sogani PC, Israel A, Lieberman PH, Lesser ML, Whitmore WF Jr (1985) Gleason grading of prostate cancer: a predictor of survival. *Urology,* ***25****(3): 223-227*.
11. Berger I, Annabattula C, Lewis J, Shetty DV, Kam J, Maclean F, *et al.* (2018) 68Ga-PSMA PET/CT vs. mpMRI for locoregional prostate cancer staging: correlation with final histopathology. *Prostate Cancer Prostatic Dis,* ***21****(2): 204-211*.
12. Gurbuz Z, Unal U, Vuruskan E, Aydamirov M, Karkin K (2025) Factors influencing Gleason score up/downgrade in radical prostatectomy. *BMC Urol,* ***25****(1): 155*.
13. Jin P, Wang X, Ding Z, Yang L, Xu C, Wang X, Huang F (2025) Development and validation of risk-stratified biopsy decision pathways incorporating MRI and PSA-derived indicators. *Ann Med,* ***57****(1): 2446695*.
14. Quarta L, Stabile A, Pellegrino F, Scilipoti P, Longoni M, Cannoletta D, *et al.* (2025) Tailored use of PSA density according to multiparametric MRI index lesion location: results of a large, multi-institutional series. *Prostate Cancer Prostatic Dis, [Epub ahead of print]*.
15. Heetman J, Pereira L, Kelder J, Soeterik T, Wever L, Lavalaye J, *et al.* (2024) The additional value of 68Ga-PSMA PET/CT SUVmax in predicting ISUP GG ≥2 and ISUP GG ≥3 prostate cancer in biopsy. *Prostate,* ***84****(11): 1025-1032*.
16. Pepe P, Pepe L, Pennisi M (2024) Negative biopsy histology in men with PI-RADS score 5: is it useful PSMA PET/CT evaluation? *Arch Ital Urol Androl,* ***96****(2): 12358*.
17. Chen M, Guo S, Wang J, Wang N, Wen S, Zhang H, *et al.* (2025) Development and validation of multivariable biopsy-free nomograms to predict clinically significant prostate cancer in patients with prostate-specific antigen levels ≥20 ng/mL. *Transl Androl Urol,* ***14****(3): 507-518*.
18. Li Y, Li J, Yang J, Xiao L, Zhou M, Cai Y, *et al.* (2025) Using a novel PSMA-PET and PSA-based model to enhance the diagnostic accuracy for clinically significant prostate cancer and avoid unnecessary biopsy in men with PI-RADS ≤3 MRI. *Eur J Nucl Med Mol Imaging,* ***52****(3): 913-924*.
19. Wang J, Chen M, Guo S, Xu Y, Liu L, Jiang X (2025) Development and validation of biopsy-free nomograms for predicting clinically significant prostate cancer in men with PI-RADS 4 and 5 lesions. *Sci Rep,* ***15****(1): 2506*.
20. Falkenbach F, Schmalhofer M, Tian Z, Mazzucato G, Karakiewicz P, Graefen M, *et al.* (2025) Size and SUVmax define the contribution of nodal metastases to PSA in oligorecurrent prostate cancer. *Prostate,* ***85****(1): 105-111*.
21. Li R, Fu Y, Peng S, Yang F, Ai S, Wang F, *et al.* (2025) Pathological and radiological features of false-positive lesions on [68Ga]Ga-PSMA-11 PET/CT in primary staging of prostate cancer: a radio-pathology matching analysis. *Eur J Nucl Med Mol Imaging,* ***52****(8): 2804-2813*.

[DOI: 10.61186/ijrr.24.2.14]